R KUMAR
A SARAVANAN
NANDEESHA H L
TEJAS N
and
ARCHITHA N

Mechanism of improved mobility of six-wheeled vehicle for mining application

Human inventions have been developing since the Stone Age. From the invention of the wheel to the progress of today's best truck. In the process of evolution, humans have improved their ability to traverse different terrains. On each occasion, due to the height and inclination of the obstacles, portability has been hampered. Most of the obstacles with a gentle slope have been effectively overcome. However, due to unstable obstacles, the vehicle did not pass through. Consider the suspension components of the 4-bar tipping bogie. To ensure the great flexibility of the bogie, the turn should be kept in a reasonably expected low position while maintaining maximum ground freedom.

To design a vehicle that can climb a 90 degree slope, the basic 4 bar tipping bogie instrument has been used with a trapezoidal front fork to give the vehicle a 90-degree slope climbing obstacle. An inflated tire can expand the vehicle's wheelbase and keep the focus of gravity on the frame even when climbing obstacles. Through the above changes, the vehicle can climb a deterrent with a height twice the width of the wheel and a lean point of 90 degrees. Using this mechanism in the mining robots can be accomplished various applications such as mining, robotic excavation, transportation, robotic surveying, robotic drilling, and handling explosives. Tipping bogie suspension will become an alternative mechanism for super terrain mining.

Keywords: Rocker bogie mechanism, mobility, 6 wheeled vehicle.

1.0 Introduction

With the post invention of the wheel, car science has developed from bullocks to beast trucks. However, the heights of the terrain cause transportation restrictions. Today a human remains at a point where he can defeat hindrances, which is 0.75 to 0.85, on occasion the wheel measurement. The versatile vehicle is a self-sufficient framework equipped for navigating a landscape with obstructions. While designing a vehicle, the designer probably decides on terrain necessities like durability, stability standards, obstacle height, and surface friction. Wheeled locomotion's fundamental segment is its suspension mechanism, which associates the wheels to the principal body (chassis). This connection can be a few different ways like springs, elastic rods, or rigid mechanisms. The majority of the substantial vehicles as if trucks use leaf springs for comfortable drive light motor vehicles are like cars that have complex spring, damping, and mechanism combinations.

Discussing obstacles, in four-wheel drive off-road vehicles, the limit is almost 50% of their wheel diameter. It is possible to pass over more than weight by accelerating the wheel to an obstacle, which is called climbing. Step climbing is the greatest furthest reaches of a car climbing (of an obstacle). While driving on a leveled surface, if there is no slipping, the wheel center will move correspondingly to the surface with a steady speed. While climbing rectangular type steps the trajectory of the wheel centers, during movement produces a soft curve, thus the horizontal motion of the wheel cater doesn't break. The mechanical linkage is a progression of rigid links connections associated with joints to frame a closed chain or a progression of closed chains. Each link has at least two joints, and the joints have different degrees of freedom to permit movement between the links. Linkages are called if two links are movable with respect to a fixed link. Thus, mechanical linkages are normally intended to take a motion and convert it into another movement as a mechanical benefit. Degrees of freedom are set of independent displacements or rotations that determine completely the distorted/deformed position and orientation of the body system.

The Rocker-Bogie component is a kind of suspension game plan that has been utilized for the Mars meanderer activities. These rockers have an inclination of showing variable relative movement to each other; they are being associated by one another just as the case by a differential. One finish of the rocker has a bogie. These largely convey the heap of the wanderer. It might contain numerous significant segments and circuit sheets that power the wanderer.

Blind peer reviews carried out

Messrs. R Kumar, A Saravanan and Ms. Nandeesha H. L, Tejas N and Architha N, Department of Mechanical Engineering, Department of Electronics and Instrumentation, MS Ramaiah Institute of Technology, Bangalore, 560054, India. e-mail: kumar4cim@gmail.com / hl.nandeesha@gmail.com

2.0 Kinematic algorithms

The forward and reverse kinematics of the rover (Rocky 8) shown in Fig. 1 are determined. The forward kinematics of the vehicle is used to estimate the movement of the rover at a given wheel speed and turning angle, bogie, and steering. The inverse kinematics of the vehicle is used to calculate the wheel speed and steering angle required to produce the required movement. These algorithms are specific to a rocker-bogie configuration with six steerable wheels (Fig.1). However, the techniques used to derive these algorithms can be applied to any vehicle configuration, although the observable degrees of freedom (d.o.f.) for different configurations may be less. Additionally, these advanced kinematics algorithms can be applied directly to the rover with a functional sub-assembly (for example, a rover rocker-bogie with only four of the six wheels capable of turning, such as the Mars Exploration Rover (MER), or only equipped with four wheels with or without joysticks, etc.) Simply limit the relevant parameters to constants. The motivation to develop the full kinematics of this type of vehicle instead of adopting the more common plane simplification is 2x. First, it allows the observation of 5 degrees of freedom, while the flat approximation limits it to 3 degrees of freedom. Second, as the terrain becomes more rugged, the error will increase due to the assumption of the plane..

These errors will be very large (up to 30% of the travel distance) and will affect the slip calculation, which in turn will affect the slip compensation driver. The forward and reverse kinematics formulas are very similar to those in references [15, 16], and the six-wheel steering has been significantly expanded.

Fig.1: Rocky 8

3.0 Rocker–bogie configuration

The rocker-bogie configuration is a commonly used suspension system for planetary probes and their prototypes. The configuration analyzed in this work includes 15 degrees of freedom: six steer/drive wheels (12 degrees of freedom), a rocker, and two bogies (all these degrees of freedom are detected by encoders or potentiometers). Describing the benefits of such a mobile system is beyond the scope of this article; interested readers refer to the references [11]. Discussion on this topic. Next, we show that under two assumptions, the rocker-bogie system allows the observation of 5 of 6 degrees of freedom. Homeless. These assumptions are: (i) the wheel/ground contact point is at a constant position relative to the axle, and (ii) the slip between the wheel and the ground only occurs around the steering axle (for example, no lateral or rolling slip). However, these slip assumptions are only applicable to motion algorithms, not to the entire slip compensation system.

3.1 The rocker bogie mechanism working

The front fork reaches on the step, compressing its spring; at that point, the energy amassed in the spring helps the first wheel of the bogie to climb. The rear wheel of the bogie is in contact with the wall, the bogie turns around the step. At that time, the center of gravity of the mechanism has arrived at nearly its final height. At last, the last wheel can get on the step with ease. The accompanying rocker-bogie mechanisms were considered to allude Fig.2. Out of the four instruments considered in Fig.2, the component is settled because of the accompanying motivation to guarantee great versatility of the bogie; the rotate should be kept up low as could be expected under the circumstances while keeping a

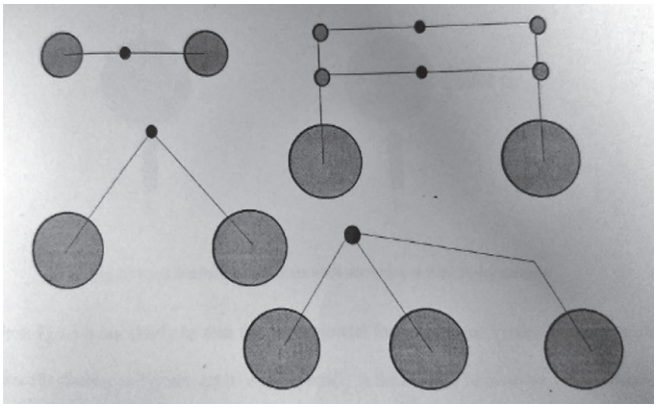

Fig.2: Rocker-bogie mechanism considered

most extreme ground leeway. With the picked, four-bar rocker-bogie component, which can effectively climb snags with a smooth bend that has a height smaller than the wheel with a slant of 90 degrees and height 1.5 to multiple times the wheel distance across, this instrument, falls flat. This will be fixed by the powers following up on the wheel when the current 4 bar rocker-bogie component experiences such an impediment with the above-given highlights (Fig.5). Let F, F1 be the power

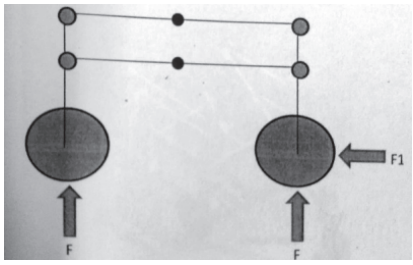

Fig.3: The Rocker-bogie mechanism chosen

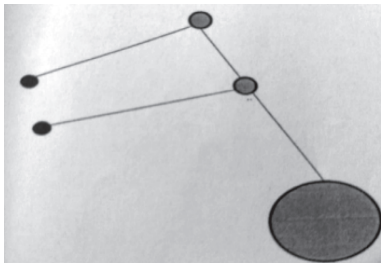
Fig.4: The extra trapezoidal arm

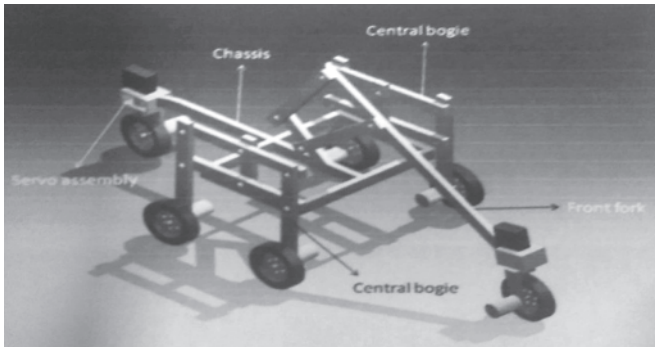

Fig.5: Isometric view of the mechanism

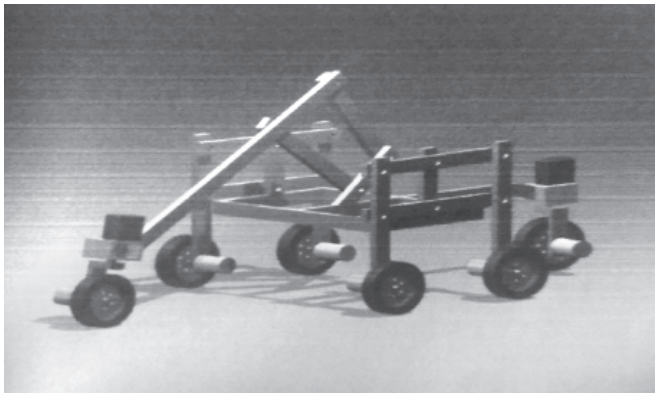
Fig.6: Side view of mechanism

demonstration when the vehicle experiences a snag with a sharp edge, which is 1.5 to multiple times the measurement of the wheel. A vertical segment of F1 is expected to make it move against the sharp edge. In this manner tends to be finished by utilizing a trapezoidal front fork that has been utilized to scale hindrances with a slant of 90 degrees allude to Fig.4.

To keep up the focal point of gravity inside the framework consistently, the vehicle eel base has been expanded by adding an additional wheel at the backside. Considering all the changes, the last instrument was created as appeared in Fig.3 and Fig.4

3.2 The expected working of the mechanism

The front fork jumps onto the progression and along these lines packing the spring in the trapezoidal front fork (appeared in Fig.5 and Fig.6. At that point, the energy amassed in the spring helps the primary wheel of the bogie to hop on to the hindrance. At the point when the back tire of the focal bogie is in contact with the divider, the bogie pivots the progression. As of now, the focal point of gravity has arrived at nearly its last stature. At last, the keep-going wheel can jump on to the progression. At that point, the last wheel iS delayed to the progression by different wheels.

Steering directing is a term applied to an assortment of parts, linkages, and so forth, which will permit any vehicle to follow the ideal course. In view of the presence of front and back tires, it is unrealistic to utilize direct pallet steer. The controlling of the wanderer was acknowledged by synchronizing the guiding of the front and back tires and the speed contrast of the bogie wheels. This takes into account high exactness moves and in any event, turning on the spot with the least slip.

3.3 Microcontroller used

Amiga 8 microprocessor

To accomplish a legitimate synchronization between the cow point and speed variety of the focal bogie wheels, a microcontroller utilized is ATMEGA 8.

B. H. bridge

Since the Arduino board gives just 5 V yield, a H-connect utilizes 5V as control signal which is utilized to control 12V DC engines.

4.0 Result and discussions

A CAD model was created in the Autodesk Inventor-10 and traded to the pressure investigation climate where the powers are broken down and the accompanying numbers are produced. Table 1 shows the basic numbers of different variables with respect to the mechanism.

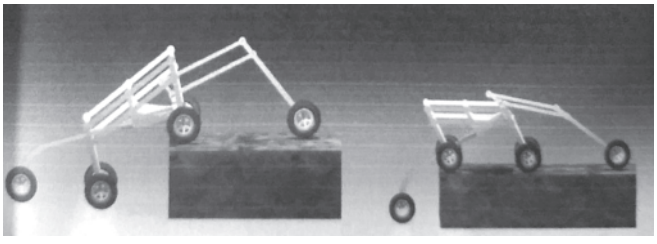
Fig.7: Expected working mechanism 1

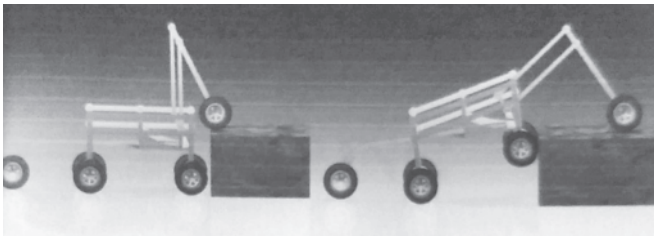
Fig.8: Expected working mechanism 2

Table 1: Basic numbers

Name	Maximum	Minimum
Volume	1342130 mm^3	-
Mass	3.63717 Kg	-
1st Principal stress	–0.878866 MPa	7.43092 MPa
3rd Principal stress	–9.40085 MPa	1.25023 MPa
Displacement	0.000000147462 mm	0.226049 mm
Safety factor	3.5 ul	3.5 ul
Stress XX	–3.439 MPa	3.45036 MPa
Stress XY	–1.94661 MPa	2.99427 MPa
Stress XZ	–1.94303 MPa	1.92104 MPa
Stress YY	–8.0138 MPa	7.03922 MPa
Stress YZ	–1.87807 MPa	2.44729 MPa
Stress ZZ	–1.94448 MPa	1.97867 MPa
X Displacement	–0.0810756 mm	0.0301694 mm
Y Displacement	–0.0186619 mm	0.214333 mm
Z Displacement	–0.0452616 mm	0.0269719 mm
Equivalent strain	0.00000000000742897 ul	0.00011098 ul
1st Principal strain	–0.0000000240778 ul	0.000097416ul
3rd Principal strain	–0.000125455 ul	0.000000088 ul
Strain XX	–0.0000490522 ul	0.000050182ul
Strain XY	–0.0000375761 ul	0.000057799ul
Strain XZ	–0.000037507 ul	0.000057799 ul
Strain YY	–0.0000995257 ul	0.0000898553ul
Strain YZ	–0.0000362531 ul	0.000047240ul
Strain ZZ	–0.000022205 ul	0.000037898ul

According to the robot motion in all the terrain conditions has been simulated in the software and possible maximum stress analysis has been completed. Stress in all the directions is calculated that has been recorded in Table 1. These stress concentrations will increase or decrease on the bogie mechanism along with a variation of the force transmitting while moving in the tough terrain. Different directional stress concentration on the bogie mechanism is simulated with the help of software (Figs.11, 12, 13 and 14). Force will be transferred to the robotic body via connecting pins and suspension systems of the individual lever. This force was also calculated on each pin and lever of the robot and recorded in Table 2.

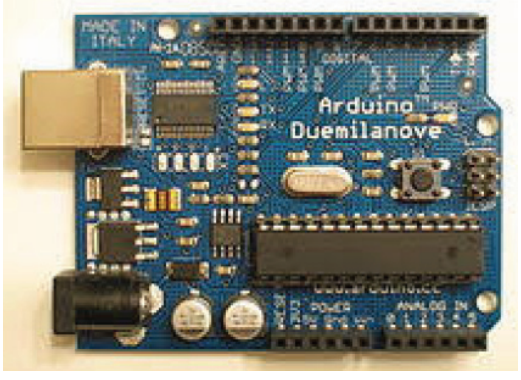

Fig.9: Arduino board with ATMEGA 8 microcontroller

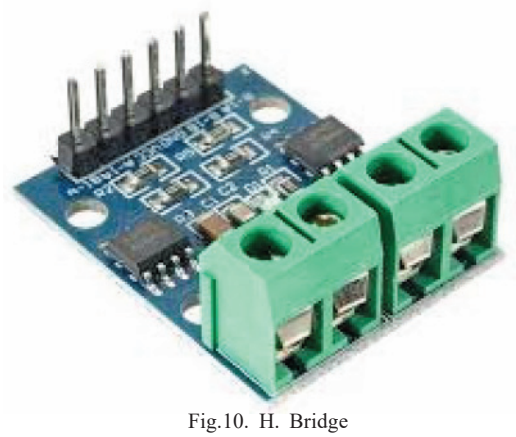

Fig.10. H. Bridge

Based on the traction force required for the robot and spring constant for the suspension system, selection criteria of the spring and motor calculation has been done in the following steps.

A. Spring calculation

From the dynamic analysis, the maximum force and corresponding deflection were found to be 32N and 20 mm respectively. Using the following values, the dimensions of the spring were calculated as follows:

For oil-tempered spring:

Ultimate Strength: τ_y =794 MPa

Modulus of torsion: G=79000 MPa

FOS=2

Hence $\tau = \tau_y/2 = 794/2=397$ MPa

(1) Diameter of the spring wire (d)

$\tau = 8FDk/\pi d^3$

Wahl's stress factor, $k = \{(4c–1)\ (4c–4)\} + \{0.651/c\}$

k = 1.1448

Therefore: 10 = D/d; D = 10d

$397 = \{(8*32*10d*1.1448)/\eth d^3$

d = 1.5mm

(2) Diameter of the coil (D)

D = 10d = 10*1.5 = 15mm

(3) Number of coils or turns (i)

Deflection $y = 8FD^3i/d^4G$

$20=\{(8*32*15*15*15*i)/(1.5^4*79000)\}$

I = 9.26 = 10

Assuming squared and ground end, n = 2

i' = i+n = 10+2 = 12

(4) Free length (I_0)

$I_0 > = (i*d) + y + a$

a = 25% of y = 0.25*20 = 5mm

$I_0 > = (12*1.5)+20+5 > = 43$ mm

TABLE 2: FORCE AND MOMENTS AT THE PIN CONSTRAINTS WITH RESPECT TO MECHANISM.

Constraint name	Reaction force		Reaction moment	
	Magnitude	Component (x, y, z)	Magnitude	Component (x, y, z)
Pin Constraint 1	29.1348 N	24.012 N	0.263616 Nm	-0.185471 N m
		-16.4992N		-0.187334 Nm
		-0.16160 N		-0.0000740757Nm
Pin Constraint 2	1.29624 N	0.62605N	0.00552593 Nm	0.00294016 Nm
		-1.13335N		0.00467878 Nm
		-0.06117N		-0.000000908499Nm
Pin Constraint 3	14.7442 N	-9.7049N	0.0787283 Nm	0.0697821 Nm
		-11.086 N		-0.03645 Nm
		-0.5543 N		$-9.08499*10^{-6}$Nm
Pin Constraint 4	14.4522 N	5.61357N	0.101577 Nm	0.100465 Nm
		-13.2501N		0.0149831 Nm
		1.33667N		-0.0000027226 Nm
Pin Constraint 5	0.659051 N	0.65513N	0.00408589 Nm	$3.50301*10^{-3}$ Nm
		-0.05245N		-0.0040784 Nm
		-0.04890N		$-8.22783*10^{-6}$ Nm
Pin Constraint6	0.41619 N	0.19955 N	0.00232455 Nm	-0.00197524 Nm
		-0.36518N		-0.00407084 Nm
		0.00604 N		0.00000168546 Nm
Pin Constraint7	0.205487N	-0.17708 N	0.00128099 Nm	0.000642078Nm
		0.06178N		-0.00110845 Nm
		-0.08395N		0.00000290546Nm
Pin Constraint 8	3.15352 N	1.4296 N	0.150443 Nm	-0.135346 Nm
		2.15757 N		-0.0656865 Nm
		1.80161 N		0.00000828941 Nm
Pin Constraint 9	11.7777 N	3.0153 N	0.0466503 Nm	-0.0449751 Nm
		-11.3433 N		0.0123894 Nm
		0.855725 N		0.00000493549 Nm
Pin Constraint 10	5.92653 N	-2.82809 N	0.089271 Nm	-0.0848577 Nm
		-4.76034N		-0.0277212 Nm
		-2.1130 N		0.0000615547 Nm
Pin Constraint11	0.38461 N	0.14871N	0.000838049 Nm	0.000420178 Nm
		-0.35437 N		0.000725097 Nm
		0.01503N		-0.00000329455 Nm
Pin Constraint 12	9.24521 N	-0.20704 N	0.0583264 Nm	0.0583127 Nm
		-9.24286 N		-0.00126462 Nm
		-0.0233831 N		0.00000169091 Nm
	0.976182 N	-0.93283 N	0.00491786 Nm	-0.00138905 Nm
		0.284865 N		0.00471761 Nm
		0.0401469 N		-0.00000419267 Nm
Pin Constraint 14	10.1632 N	-7.02471 N	0.121093 Nm	0.0874679 Nm
		7.23462 N		0.0837435 Nm
		1.2667 N		-0.0000965311 Nm
Pin Constraint 15	0.957082 N	0.794526 N	0.00620769 Nm	0.00408197 Nm
		-0.527794 N		0.0467685 Nm
		-0.0785339 N		-0.000000190728 Nm
Pin Constraint 16	14.9361 N	8.55308 N	0.0483004 Nm	0.0267165 Nm
		-12.0508 N		-0.0402388 Nm
		-2.17077 N		-0.000000980942 Nm
Pin Constraint 17	9.24521 N	-0.207049 N	0.0583264 Nm	0.0583127 Nm
		-9.24286 N		-0.00126462 Nm
		-0.0233831 N		0.00000169091 Nm
Pin Constraint18	10.1632 N	-7.02471 N	0.121093 Nm	0.0874679 Nm
		7.23462 N		0.0837435 Nm
		1.2667 N		-0.0000965311

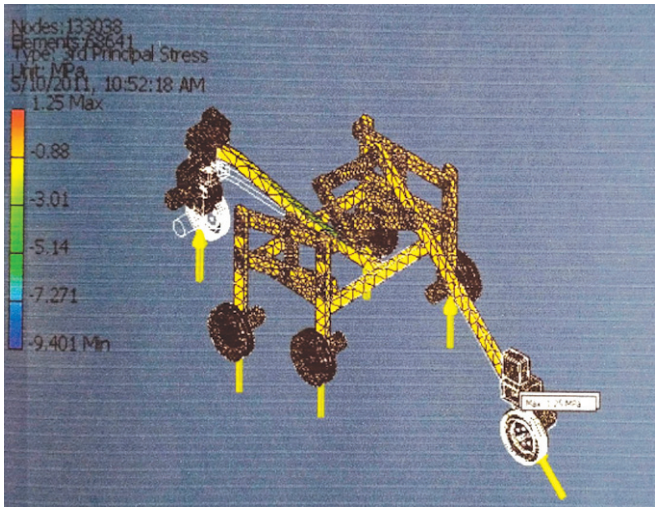

Fig.11: Principle stress

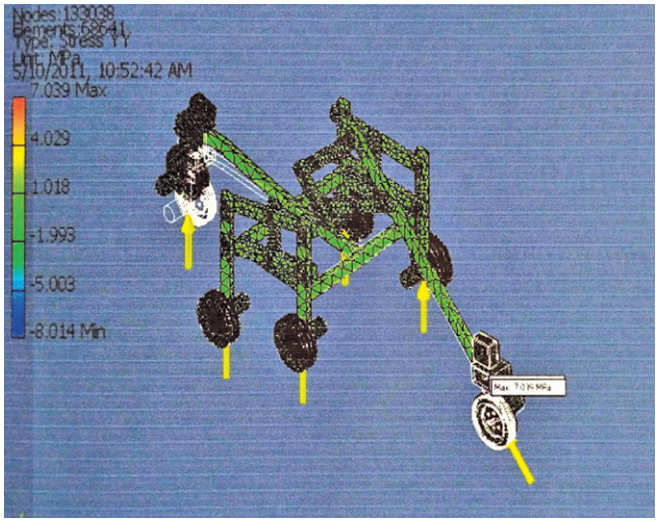

Fig.12: stress XX

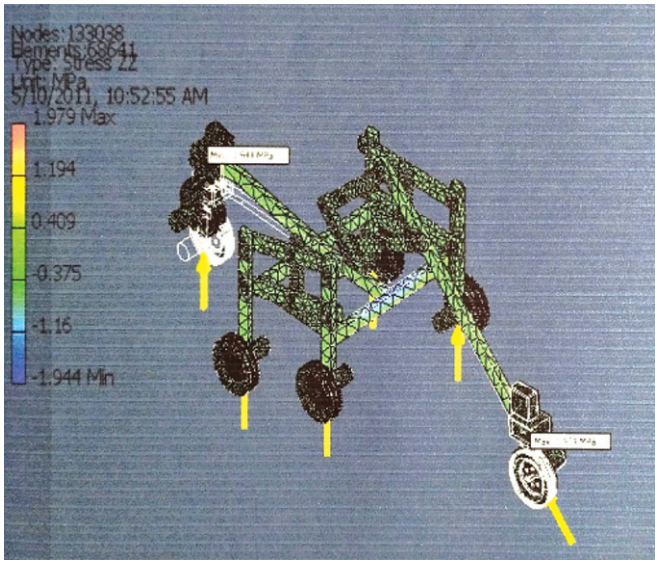

Fig.13: stress YY

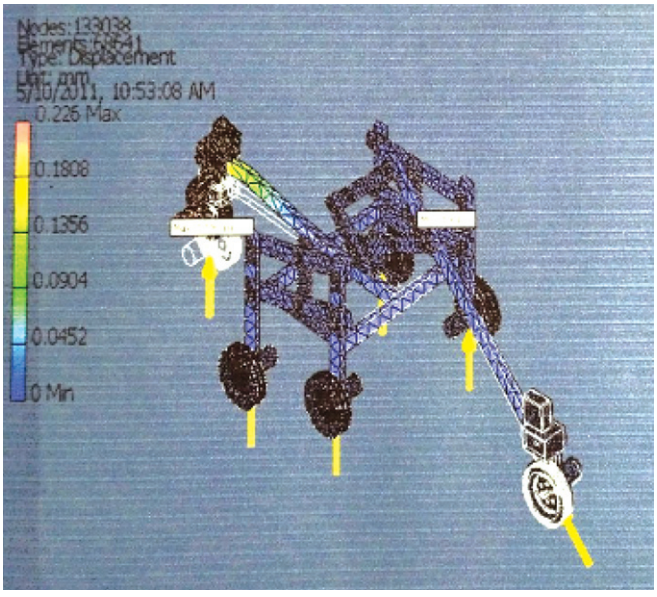

Fig.14: stress ZZ

(5) Pitch (p)

$p = (i_0\text{-}2d)/i = 40/10 = 4mm$

(6) Stiffness (F_0)

$F_0 = F/y = 32/20 = 1.6$ N/mm

B. Power calculation

The intensity of the accessible engines was checked for prior to utilizing it in the model. To discover the force we utilize an arrangement (Fig.15) which has a realized burden applied at the shaft and the time taken by the engine to move the heap per unit distance was recorded to figure the force.

V_{avg} from the above observation table = 0.016305 m/s

$P = F^* V_{avg}$

0.5*9.81*0016305 = 0.07997 Nm/s

For 6 motors P = 6*0.07997 = 0.479856 W

W = 5kg {3.6+1.4(1.4 is assumed to be the weight of the board and other platforms)}

V = 0.479856/50

= 0.0095797 m/s

= 0.9597 cm/s

Since the same torque will be used to drive the robot, calculated driving system is used in the robot for traction purpose.

C. Steering calculation

For the directing reason we utilize an Arduino board which can be utilized to accomplish legitimate synchronization between the cow point and speed varieties. For 225 varieties in the control signal that PWM (pulse width modulation) pins on the Arduino board are fit for giving 90 distinct yields that steer the servo engines.

Table 3: Observation

Time (Seconds)	Distance (meters)	Velocity (meter/second)
12	0.195	0.01625
11	0.18	0.01636
12	0.194	0.01616
12	0.195	0.01625

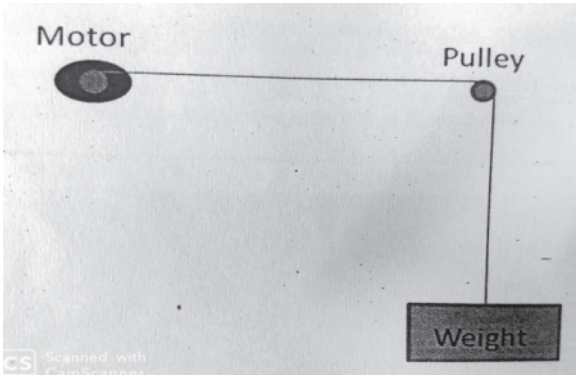

Fig.15. Power calculation setup

Fig.16: Final model developed

Inner wheel speed (new) = Inner_wheel_speed (old) – ((225/90) *(servo_steer_angle –90))

This above formula was used in the coding of the steering of the servo motor.

From the above numerical calculation, the components used to fabricate the six-wheeled mechanism and power requirement were validated and it was used to programme the microcontroller for its smooth operation.

4.0 Conclusions

The mechanism designed in this research work will improve the impediment-climbing limit of 6 wheeled vehicles which can be used in mining and other applications.

The proposed structure in the mechanism can be utilized as a base for mountings like an automated arm, wheel seat, payload lodge, radar, spy cameras, etc. Which can be utilized for mining applications like mapping, survey, dozing, and haulage.

The mechanism developed can be used as follows

(1) Fire fighting
(2) Rescue missions during catastrophe
(3) Remote inspection
(4) Space exploration
(5) Assisted handicapped stair climbing wheel chair
(6) Unmanned ground vehicle (UGV)
(7) With the help of modifying the onboard electronic components, it can be used as a robot with the following features:
- Autonomously navigate through collapsed structures
- To find their victims and ascertain their condition
- Produce practical maps of their location
- Identify hazards

Nomenclature

τy =Ultimate strength

G = Modulus in torsion

F = maximum force acting on the spring

Y = Corresponding deflection of the springs at maximum force

i = number of coils or turns

n = squared and ground end

i' = Total number of turns

a = clearance

I0 = Free length

p = Pitch

F_0= Stiffness

d = Diameter of the spring wire

D = Diameter of the spring coil

T = time in seconds

S = Distance in meters

V = velocity in m/s

Vavg = Average velocity

References

[1] Thomas Thueer, Ambroise Krebs, Roland Siegwart, (2006): "Comprehensive locomotion performance Evaluation of All-Terrain Robots," Proceeding of the 2006 IEEE/RS International Conference on Intelligent Robots and Systems, Beijing, China, pp. 4260-4265, Sep, 2006.

[2] Volpe R., Balaram J., Ohm T. (1996): "The Rocky 7Mars Rover Prototype," IEEE International Conference on Intelligent Robots and Systems, pp.1558-1564 , Mar, 1996.

[3] Brian D, Harrington, Chris Voorhees, (2004): "The

Challenges of Designing the Rocker-Bogie Suspension for the Mars Exploration Rover," Proceedings of the 37th Aerospace Mechanisms SymposiumÿJohnson Space Center.

[4] Panigrahi P., Barik A., Rajneesh R. & Sahu R. K. (2016): "Introduction of Mechanical Gear Type Steering Mechanism to Rocker Bogie", *Imperial Journal of Interdisciplinary Research* (IJIR) Vol.2, Issue-5, ISSN: 2454-1362.

[5] BaresJ., Wettergreen D. (1997): "Lessons from development and deployment of Dante II". Proceedings of the 1997 Field and Service Robotics Conference, December.

[6] Lauria M, Conti F, Maesuli P. A., Van MInnendael., Bertrand R., Siegwart R. (1998): "Design and Control of an Innovative Micro-Rover", Proceedings of 5th ESA Workshop on Advanced Space Technologies for Robotics and Automation, The Netherlands.

[7] Bergemann D. and Välimäki J. (2002), "Information and Efficient Mechanism Design", *Econometrica*,70,1007-1033

[8] Design of a Mars Rover Suspension Mechanism by Firat Barlas. Introduction to Robotics by John J. Craig - Pearson/Prentice Hill (2005)

[9] Design of Machine Elements – 2 Textbook by JBK Das & PLS Murthy, 2004 Edition.

[10] Bhole, A., Turlapati S. H., Rajashekhar V. S, Dixit J., Shah S. V., Madhava Krishna K, (2016): "Design of a Robust Stair Climbing Compliant Modular Robot to Tackle Overhang on Stairs" arXiv:1607.03077v1 [cs.RO], 11 Jul 2016.

[11] Yadav, N. Bhardwaj, B., Bhardwaj, S. (2016): "Design analysis of Rocker Bogie Suspension System and Access the possibility to implement in Front Loading Vehicles", *IOSR Journal of Mechanical and Civil Engineering,* e-ISSN: 2278-1684, p-ISSN: 2320-334X, Volume 12, Issue 3 Ver. III, PP 64-67, May-Jun. 2015.

[12] Olson C. F., Matthies L. H., Shoppers M. and Maimone M. (2001): Stereo ego-motion improvements for robust rover navigation, in: Proc. IEEE Int. Conf. on Robotics and Automation.

[13] Cheng Y., Maimone M. and Matthies L. (2005): Visual odometry on the Mars Exploration Rovers, in: Proc. IEEE Conf. on Systems, Man and Cybernetics, The Big Island, HI.

[14] Thomas George and Vladimir V. Vantsevich. (2010): Wheel-terrain-obstacle interaction in vehicle mobility analysis. Vehicle System Dynamics, 48:S1, 139-156, DOI: 10.1080/00423111003690496. Published online: 26 Nov.

IMPACT FACTOR IMPROVEMENT AND MAINTENANCE SCHEDULE OPTIMISATION OF MINING SHOVELS BY REMAINING USEFUL LIFE AND LINEAR PROGRAMMING

(Continued from page 326)

35. Peralta, S., Sasmito, A. P., and Kumral, M. (2016): Reliability effect on energy consumption and greenhouse gas emissions of mining hauling fleet towards sustainable mining. *Journal of Sustainable Mining*, 15(3), 85–94.

36. Prytz, R., Nowaczyk, S., Rögnvaldsson, T., and Byttner, S. (2015): Predicting the need for vehicle compressor repairs using maintenance records and logged vehicle data. *Engineering Applications of Artificial Intelligence,* 41, 139–150. https://doi.org/https://doi.org/10.1016/j.engappai.2015.02.009

37. Samanta, B., & Banerjee, J. (2002): Improving Productivity of Mining Machinery through Total Productive Maintenance.

38. Samatemba, B., Zhang, L., and Besa, B. (2020): Evaluating and optimizing the effectiveness of mining equipment; the case of Chibuluma South underground mine. *Journal of Cleaner Production*, 252, 119697. https://doi.org/https://doi.org/10.1016/j.jclepro. 2019.119697

39. Sharma, N. R., Agrawal, H., and Mishra, A. K. (2019): Maintenance schedules of mining hemm using an optimization framework model. *Journal Europeen des Systemes Automatises*, 52(3). https://doi.org/10.18280/jesa.520303

40. Stahl, P., Donmez, B., and Jamieson, G. (2011): A field study of haul truck operations in open pit mines. In Proceedings of the Human Factors and Ergonomics Society Annual Meeting (Vol. 55, pp. 1845–1849).

41. Susto, G. A., Schirru, A., Pampuri, S., McLoone, S., and Beghi, A. (2015): Machine Learning for Predictive Maintenance: A Multiple Classifier Approach. *IEEE Transactions on Industrial Informatics*, 11(3), 812–820. https://doi.org/10.1109/TII.2014.2349359

42. Topal, E., and Ramazan, S. (2010): A new MIP model for mine equipment scheduling by minimizing maintenance cost. *European Journal of Operational Research*, 207(2), 1065–1071.

43. van Nunen, K., Li, J., Reniers, G., and Ponnet, K. (2018): Bibliometric analysis of safety culture research. *Safety Science*, 108, 248–258.

44. Vayenas, N., and Wu, X. (2009): Maintenance and reliability analysis of a fleet of load-haul-dump (a) vehicles in an underground hard rock mine. *International Journal of Mining, Reclamation and Environment*, 23(3), 227–238.

45. Wang, P., Li, Y., and Reddy, C. K. (2019): Machine learning for survival analysis: A survey. *ACM Computing Surveys* (CSUR), 51(6), 1–36.

Printed by Pradip Kumar Chanda at The Indian Press Pvt. Ltd. 93A Lenin Sarani, Kolkata 700 013 and published by him for Books & Journals Pvt. Ltd. from 62 Lenin Sarani, Kolkata 700 013.